Projective geometric model for automatic determination of X-ray-emitting source of a standard radiographic system

Laura García-Ruesgas*

University of Seville, Department of Engineering Graphics. Isla de la Cartuja, Camino de los Descubrimientos, s/n, Sevilla 41092, Spain.

Rafael Álvarez-Cuervo

University of Oviedo, Department of Construction and Manufacturing Engineering. Campus de Gijón, Gijón 33203, Spain.

Francisco Valderrama-Gual

University of Seville, Department of Engineering Graphics. Isla de la Cartuja, Camino de los Descubrimientos, s/n, Sevilla 41092, Spain.

José Ignacio Rojas-Sola

University of Jaen, Department of Engineering Graphics, Design and Projects. Campus de las Lagunillas, s/n. Jaén 23071, Spain.

* Corresponding author

University of Seville. Isla de la Cartuja, Camino de los Descubrimientos, s/n, Sevilla 41092, Spain.

Telephone: 34 (954) 486161 E-mail: lauragr@us.es

This is the accepted version for publication of the manuscript published in Computers in Biology and Medicine. Please, cite the published version.

García-Ruesgas, L; Álvarez-Cuervo, R; Valderrama-Gual, F; Rojas-Sola, JI. Projective geometric model for automatic determination of X-ray-emitting source of a standard radiographic system. *Comput. Biol. Med.* 2018; **99:** 209-220. DOI: https://doi.org/10.1016/j.compbiomed.2018.06.016

Projective geometric model for automatic determination of X-ray emitting source of a standard radiographic system

ABSTRACT

Background and objective: Currently, many orthopedic operations are planned by analyzing X-rays. The exact position of the focus is needed to calculate the real size of an object that is represented in conical projection, although in practice, this position is difficult to determine using current X-ray commercial systems. In this paper, a new geometric model is proposed in order to determine accurately, practically, and economically the location of the emitting source of commercial imaging systems using a single standard X-ray image.

Method: The method requires a specific reference locator object to be positioned in the visual field of radiographic image. Because this object cannot implement ideal geometric points, but instead works with small spheres, it was necessary to experimentally validate the proposed methodology. The implemented software that was developed to validate the model was used in four series of tests. In these tests, we studied the influence on the final result of: 1. the selection of a specific set of markers in radiography, 2. the focus position variation in relation to radiograph and 3. the possible rotated angle of locator object about Z axis.

Results: The results for 164 tests that were performed with this software showed that the expected error for 99.5% of values ranges with maximum error of [-0.35%, +0.39%], which shows that the model is independent of the design of locator object and its position and orientation in the radiographic field. The software used to validate the proposed model has been found useful to verify its reliability, effectiveness, ease of implementation, and accuracy.

Conclusions: This model is effective to calculate the precise position of the X-ray focus of any standard radiographic system accurately.

Keywords: projective geometric model, X-ray focus emitter, standard radiograph, specific locator reference object, MATLAB.

1. Introduction

Currently, total knee arthroplasty is an efficient and reliable approach in orthopedic surgery [1,2]. Most surgery patients report satisfactory functional results and significant pain reduction, thus notably improving their quality of life [3]. Therefore, the number of primary and revision prostheses in recent years has increased markedly, especially in younger patients [4], and implant survival is estimated at 92.3% at 15 years after surgery [5].

A common procedure used in preoperative planning [6] of knee replacements consists of analyzing X-rays previously made for the patient. In view of the daily nature of hip and knee arthroplasties, it is becoming increasingly important to make accurate measurements on standard radiographic images in order to perform postoperative surveillance [7], to improve the design of prosthetic systems [8], to perform clinical studies concerning implants reliability which assess their possible wear or deterioration over time [9,10] or to determine the variation of the relative position of the prosthetic elements over long time periods [11].

In daily work, many analyses of radiographs are performed by measuring on them directly or by using two or three-dimensional overlapping templates, in order to determine by visual comparison, the optimal size of the implant to be inserted [12]. Despite being imprecise, the measurements with templates help surgeons adapt the knee implants and align the joint properly [13].

An inherent problem in these methods is that X-rays do not show the real size of radiographed objects, because the image is generated by conical projections. This involves the loss of information needed to perform certain studies [14], leading to the use of more costly techniques such as Computed Tomography (CT) [15] or Roentgen

Stereophotogrammetry Analysis techniques (RSA) [16], which also expose the patient to higher doses of radiation.

The pinpointing of the X-ray focus position will enable these studies to be undertaken economically and with the necessary precision.

In this paper, we propose a new projective geometric model to determine accurately the position in space of the emitting source of X-rays (X-RFE, X-Ray Focus Emitter) of a standard commercial radiographic system, i.e. to specify the ideal geometric point from which radiation of X-ray commercial tube is emitted. The commercial radiographic systems used in industrial and medical applications do not permit to determine the position of the focus with the accuracy required to perform high precision measurements on radiographed objects. The problem is the X-ray emitting tubes emit radiation from an inaccessible point inside a glass flask. In addition, tubes are placed inside lead capsules in order to avoid radiation leaks and their position, in relation to X-ray machines, prevent any attempt to measure the position of focus directly.

The proposed model works with radiographic images which were made with standard systems, (i.e. with a single focus), unlike RSA analysis systems, which require special radiographic machines with two focuses that act simultaneously. In practice, most hospitals do not have RSA systems because of their high price.

All development of the proposed model is based on geometry that is associated with conical projection and classic concepts of homography have been applied.

As it is known, it is essential to place a specific reference locator object in the visual field of radiographic image to restore the focus position in relation to projection plane. Because of the fact that, in practice, it is impossible to implement ideal geometric points, it was necessary to experimentally validate the proposed model and we used

small tantalum spheres for that. Tantalum was used because it is a radio opaque and physiologically inert material which is often used in medicine field.

So therefore, the objectives of this research are:

- First of all, to develop a geometric model that can be implemented as a practical computer program, for the accurate determination of Cartesian coordinates of the X-ray emitting source of any standard radiographic system.
- To ensure that the aforementioned model can be applied in systems with a single X-ray source and in experimental situations using a single radiographic image.
- To design a specific Locator Object of Reference Markers composed of small tantalum spheres suitable for calculating the position of the focus of a radiation system from a single standard radiographic image.
- The geometric model should be independent of Locator Object of Reference Markers used [17], as well as its position and orientation, considering the limitations of geometric arrangement of its markers and its number.

2. Materials and Methods

2.1 Geometric foundation

It is proposed as a methodology to structure the development of the geometric model the 'projective unity' [18]. This methodology consists of the necessary minimum elements to define the conical projection of a point of the three-dimensional space: the focus or projection center, X-RFE, which is the reference point from which the conical projection is made, a marker –in theory, the O point of the space of the geometric center of said marker- and its $\phi(O)$ projection on the projection plane (the radiographic image). The proposed problem satisfies the way homography is set out partially, so some of its equations are applied in the development of the projective model.

The coordinates (x,y) of the projected points are known in relation to a specific point of the plane, in the proposed case, the upper left corner of the radiograph. A single projective unit cannot determine the three coordinates of the projection center and hence more than one will be needed. Specifically, according to the principles of the homography, in order to restore an object, at least four projective units must be considered and the relative distances between four points of the object and their corresponding projections have to be known.

The mathematical development requires a series of points distributed in space for which the coordinates are known in relation to a given reference system to be determined. Thus, the aim is to find the focus of a conical projection from the relative distances between points in space and the relative distances between the projections of these points. Initially, the position of points in space is arbitrary. To simplify, the origin of coordinates has been placed in the projection center.

Since only relative distances between points will be considered, any point that is incorporated must be defined according to the first point O. Therefore, the distance h is to be determined in relation to the radiograph plane, and the coordinates of the point O (O_1, O_2, O_3) in relation to focus, which is the origin of the coordinates. This information will allow to position the radiograph in relation to focus since coordinates of its upper left corner (X_rd, Y_rd , h) will be known. Once the first point O has been selected, the three needed rest points P_1, P_2 and P_3, whose coordinates may be any one at first must be selected (figure 1).

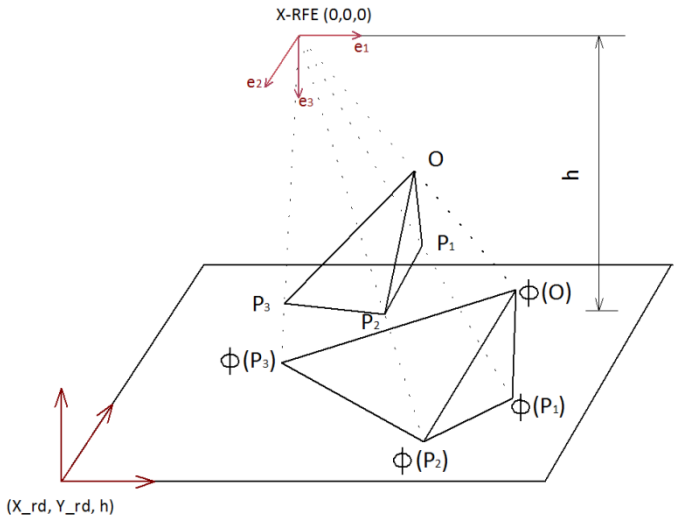

Figure 1. General sketch of the proposed problem

The relative distances between the last three selected points in relation to the first one O are known:

$$P_i - O = (p_{i1}, p_{i2}, p_{i3}); i = 1, 2, 3 \quad (1)$$

Distances between points projections of the object are also known:

$$\phi(P_i) - \phi(O) = (q_{i1}, q_{i2}, q_{i3}); i = 1, 2, 3 \quad (2)$$

These distances will be our only starting data and they will be measured in the radiograph.

The parametric equation of the line through two points will be used as a mathematical model of each projective unity. This equation is very simplified because the origin of coordinates was placed in the focus:

$$\begin{aligned} x &= 0 + \lambda x_1 \\ y &= 0 + \lambda x_2 \\ z &= 0 + \lambda x_3 \end{aligned} \quad (3)$$

As the plane is located at a height h in relation to focus, z = h and therefore λ = h/x3:

$$\phi(X) = \left(\frac{hx_1}{x_3}, \frac{hx_2}{x_3}, h\right) \quad (4)$$

It is necessary to express the coordinates of the points according to the known and unknown values.

$$\phi(P_1) - \phi(O) = \left(\frac{O_1 + p_{11}}{O_3 + p_{13}}\, h - \frac{O_1}{O_3}h, \frac{O_2 + p_{12}}{O_3 + p_{13}}\, h - \frac{O_2}{O_3}h, 0\right) = (q_{11}, q_{12}, 0)$$

$$\phi(P_2) - \phi(O) = \left(\frac{O_1 + p_{21}}{O_3 + p_{23}}\, h - \frac{O_1}{O_3}h, \frac{O_2 + p_{22}}{O_3 + p_{23}}\, h - \frac{O_2}{O_3}h, 0\right) = (q_{21}, q_{22}, 0) \quad (5)$$

$$\phi(P_3) - \phi(O) = \left(\frac{O_1 + p_{31}}{O_3 + p_{33}}\, h - \frac{O_1}{O_3}h, \frac{O_2 + p_{32}}{O_3 + p_{33}}\, h - \frac{O_2}{O_3}h, 0\right) = (q_{31}, q_{32}, 0)$$

Thus, there are six equations and only four unknown values, so that beforehand it might be assumed that two equations would be not needed, i.e. the fourth point. However, it is necessary to select a fourth point because, in order to calculate the rotation angle between the two coordinates systems used easily, it would be suitable if the first two points were selected on a plane parallel to the projection plane. Thus p_{13}=0 and the first two equations are greatly reduced. As it can be seen, these equations are redundant since they provide the same information, that is, the ratio h/O_3 and therefore, the fourth point is needed.

$$q_{11} = \frac{p_{11}}{O_3}h$$

$$q_{12} = \frac{p_{12}}{O_3}h \quad (6)$$

It should be noted that both q_{11} and q_{12} are included in the system of equations because, although they provide the same information, the chosen points are not known beforehand and there is a possibility that the two first selected points had the same coordinate X or Y.

Therefore, the solution to the problem set out requires only five of the six equations shown in (5). With respect to the first five, for example, the system of equations that determines the position in space of the emitting focus of a standard radiographic system is, therefore q_{11}, q_{12}, q_{21}, q_{22} and q_{31}.

There are two conditions that should be considered while using this methodology which are direct consequence of the adopted simplifications but do not imply restrictions of real use due to the design of the locator object. These are:

At least three markers of the locator object can not belong to the same plane parallel to the projection plane and, the third and fourth selected points must not be in the same vertical. In these situations, the system of equations has no solution but the implemented software considers both conditions as warnings for the user.

2.2 Design of the locator Object of Reference Markers

In order to implement the proposed model, a prototype of locator object was designed according to model requirements. A structure with two parallel planes to the projection plane and two perpendicular planes to said plane were arranged.

The result has a simple configuration, like a box, within which the four spheres were located. However, after several tests were made with this structure, some problems were detected: sometimes the projection of some of these spheres did not fall within the limits of radiograph. In other cases, it was verified that these projections were hidden behind bone tissue and, in some tests, it was also noticed that the spheres were projected too close together to distinguish them.

Thus, after studying several options, we chose to incorporate in the locator object prototype more spheres that needed, which were distributed as a rectangular array along the structure. This guaranteed the scanning of an adequate number of markers on the radiograph. Finally, nine markers were placed on each plane to ensure the selection on radiograph of the four required markers which implement the model.

The projection of radiological markers of the four locator object planes are displayed on radiographs as a set of points that can be difficult to identify. Therefore, the markers were distributed in a rectangular array and they were aligned in two directions. Parallel

and perpendicular lines were traced and these were screened in the same way in the planes parallel to the projection plane. In non-parallel planes to the projection plane such properties were not maintained. The distribution of points in this way still presented some confusion with respect to the identification of the locator object marker with a particular point projected on the radiograph. To solve this problem, we implemented what we called “significant points” which establish a visual reference, two close markers on the bottom plane and three close markers on one wing (figure 2).

Figure 2. Isometric perspective of locator object design

2.2.1 Materials

The structure bearing the spherical markers was manufactured in a plastic material of high mechanical strength, i.e. polymethylmethacrylate. This thermoplastic material is transparent to X-rays. Markers are spheres of tantalum which were purchased from a Swedish company.

2.3 Simulation

Before the prototype was manufactured, it was tested by virtual simulation using computer-graphics techniques (Autodesk 3ds Max) that simulate the environment of a

radiographic system [19]. The result was called “synthetic or virtual radiograph”, suitable for determine the accuracy of the developed model. This simulation allowed to optimize the design of the locator object and to validate the model virtually (figures 3 and 4).

2.4 Field tests

After virtual validation of the locator object, field tests were performed under real conditions. These were made possible thanks to the assistance of San Agustín hospital in Avilés (Spain), where several radiographs were taken in patients who had knee implants (figure 5).

It was important to verify that the locator object, which was radiographed at high intensity together with metallic and plastic implants, was behaved correctly and the methacrylate of its structure did not appear on radiographs. It was possible to verify how the markers could be seen through polyethylene inserts, but not through metal implants (figure 6).

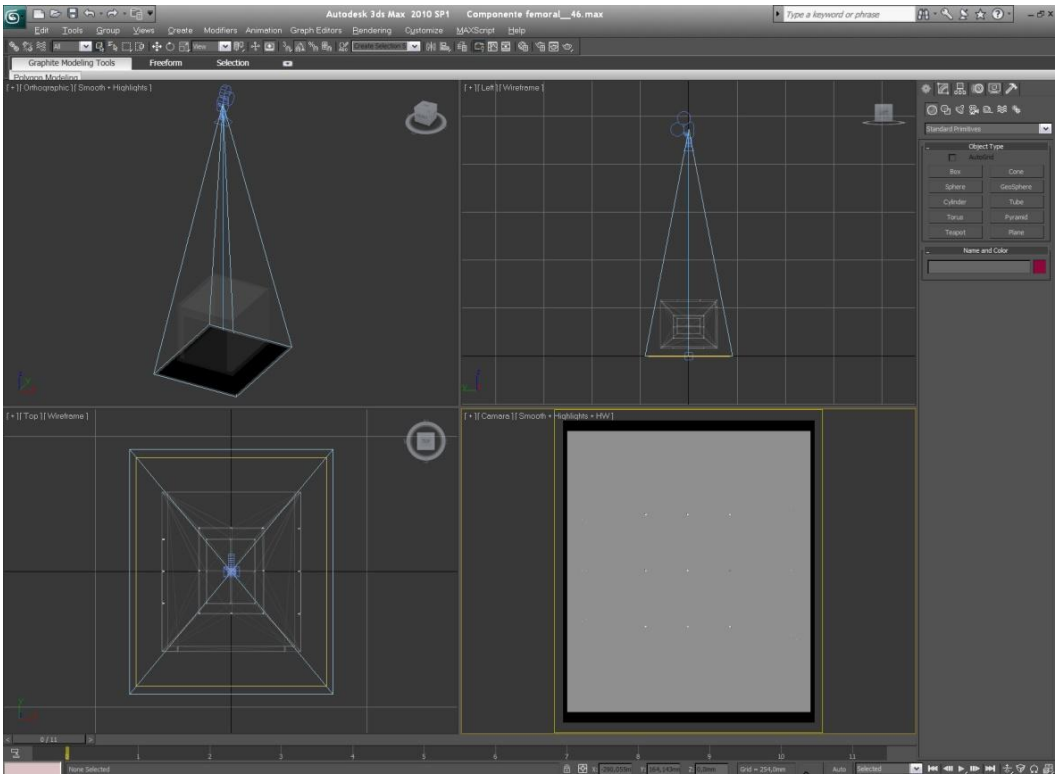

Figure 3. X-ray emitting source simulation

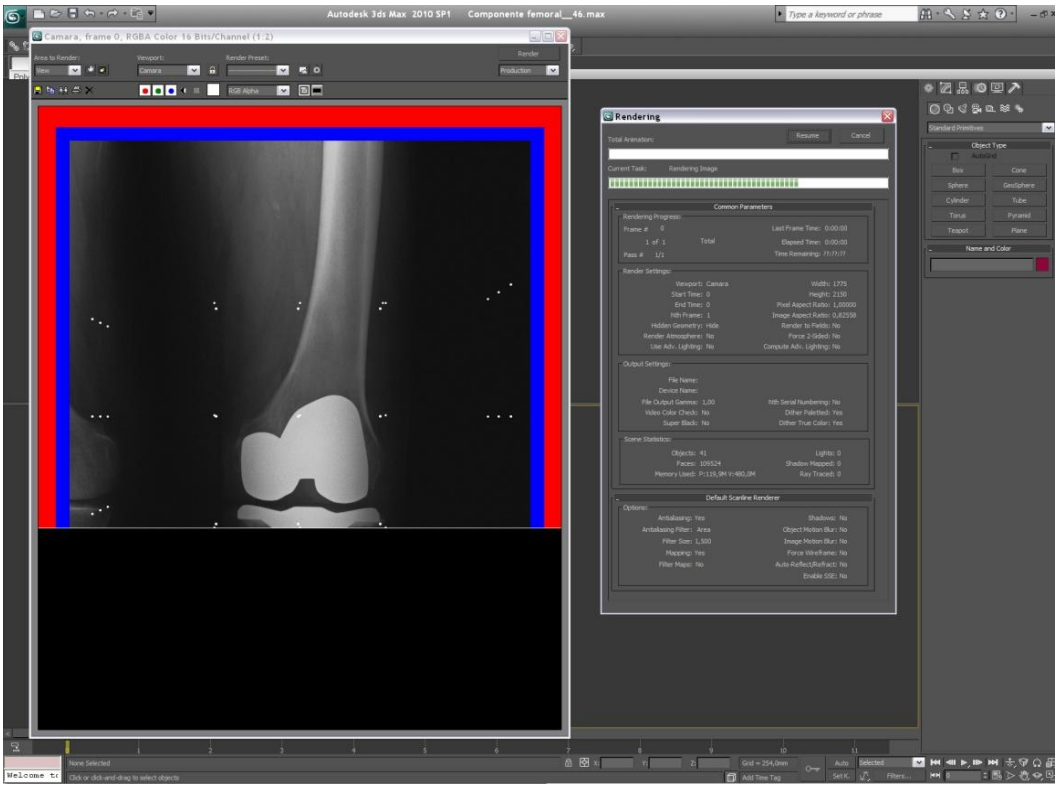

Figure 4. Virtual radiograph

Figure 5. Prototype of locator object and X-ray system

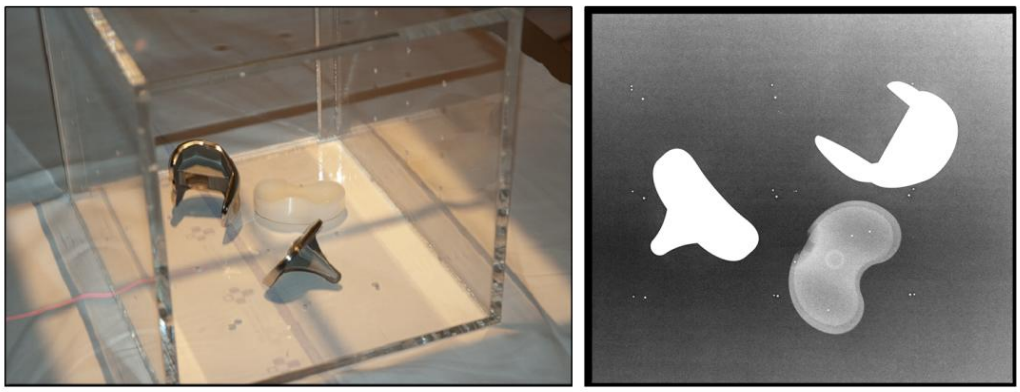

Figure 6. Behaviour of locator object and metallic and plastic implants at high radiation

2.5 Projective geometric model implementation

For the validation, the model was implemented as general-use software with MATLAB® [20]. This software was called LEFERX and it is a modular program which operative blocks can be seen in the flow chart of figure 7. This software will allow to do field tests of model and will enable the clinician or radiologist to gather the desired information quickly and easily.

Starting data is a digitized radiograph that the program can open. After opening radiograph, the program shows it in screen and allows the four needed markers can be selected. Afterwards, radiograph resolution must be input (in pixels per millimeter) [21] and then, the program will be able to apply the mathematical model and calculate the position of radiograph in relation to focus. The remainder blocks of the program are auxiliary functions that allow to save or to recover other cases of study.

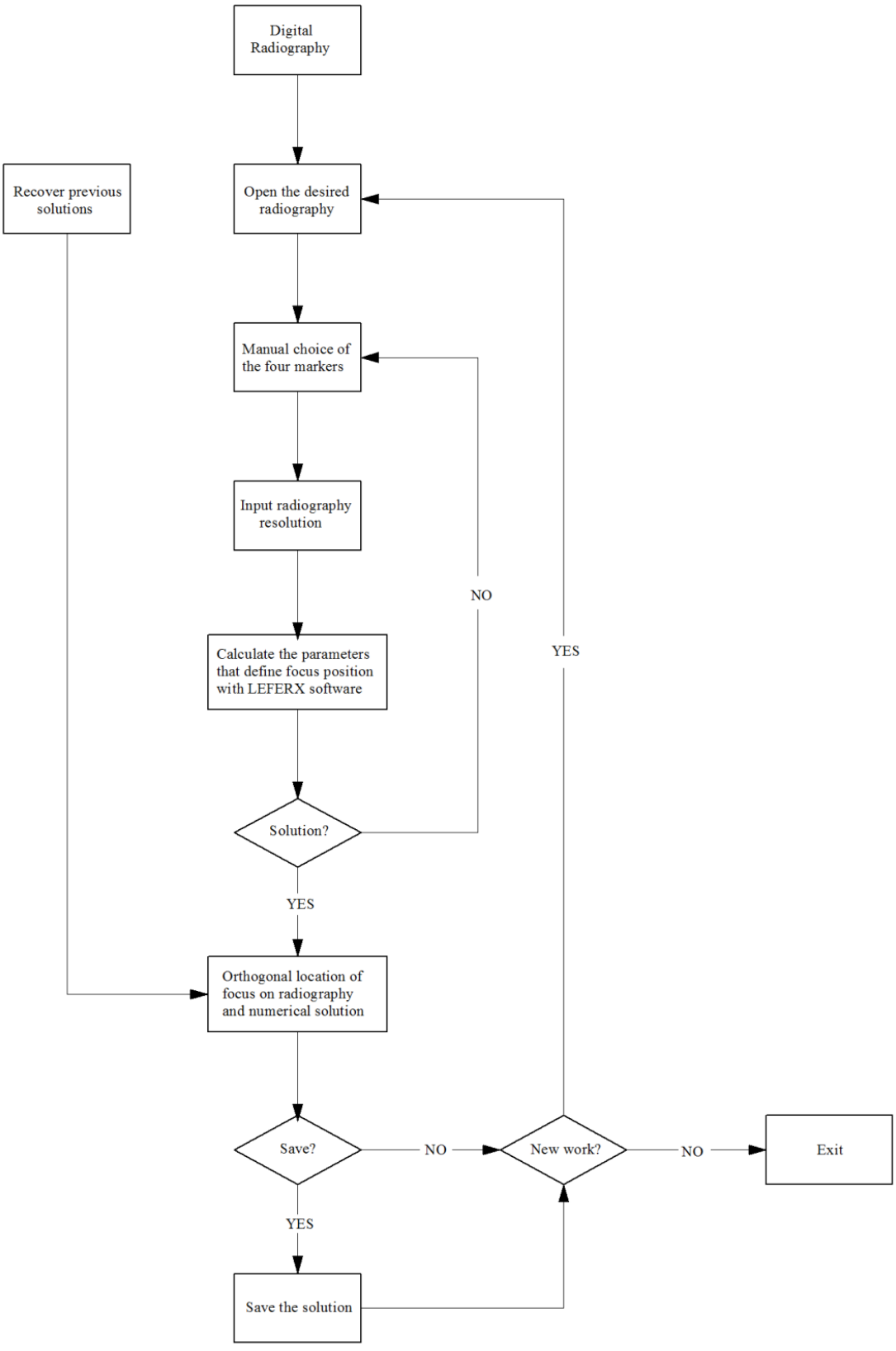

Figure 7. Flow chart of software application

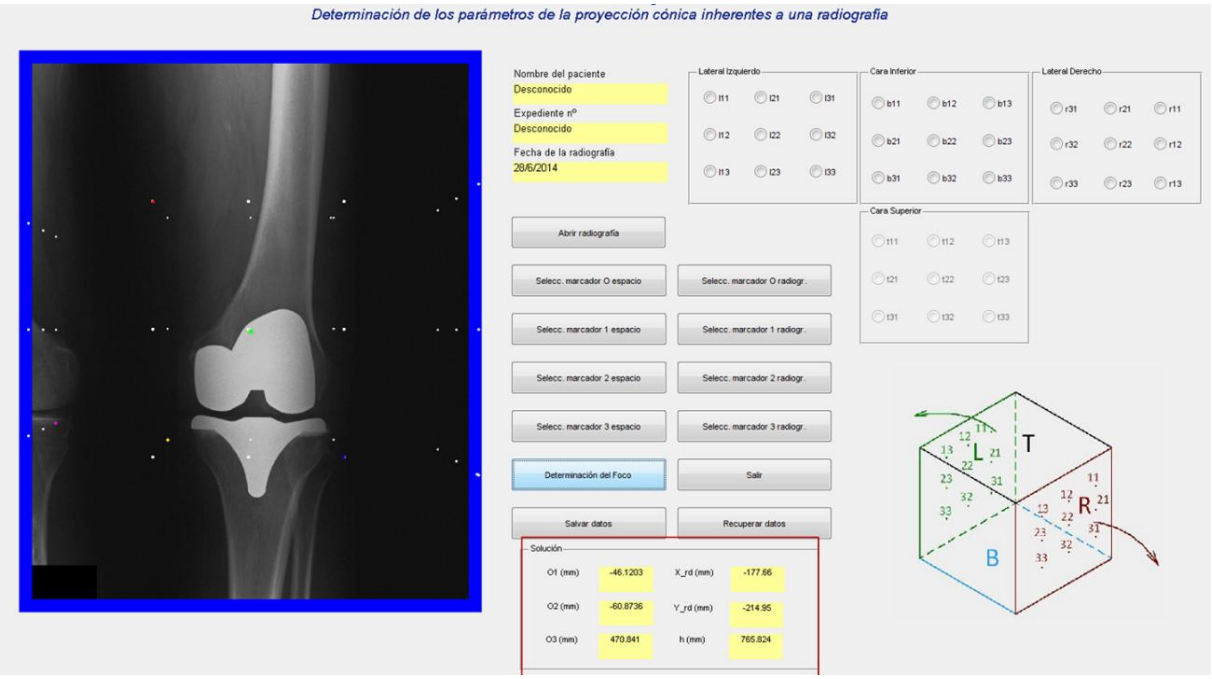

Figure 8. LEFERX interface displaying focus coordinates

A special feature to consider when calculation is done is that two different reference systems are used. The first one, absolute reference system, has its origin of coordinates in the focus, while the second, relative reference system, has the origin of coordinates in the upper left corner of the radiograph. Projections of selected markers are chosen in this last system.

It is taken into account that directions of locator object contour, match up with directions of the absolute reference system. Axes directions of this system are known on radiograph because they are aligned with the arrays of markers located at the top and underside of locator object. Axes directions of relative reference system are parallel to radiograph´s contour.

Both reference systems must be moved to the first chosen marker to solve the model. This allows to calculate the existing rotated angle between both systems which must be taken into account to calculate focus coordinates. To this end, it is necessary to transform the relative distances calculated in relation to relative reference system, into distances in relation to absolute reference system (algorithm). Radiograph resolution is

also needed. Once focus position is calculated in space, its orthogonal projection is displayed on radiograph (figure 9). If we denoted the rotated angle as α, then the coordinates on the axes of the absolute reference system (x and y) would be calculated as follows in relation to the coordinates of the axes of the radiograph (x' and y'):

$$x = x' \cdot cos\alpha + y' \cdot sen\alpha$$
$$y = y' \cdot cos\alpha - x' \cdot sen\alpha \quad (7)$$

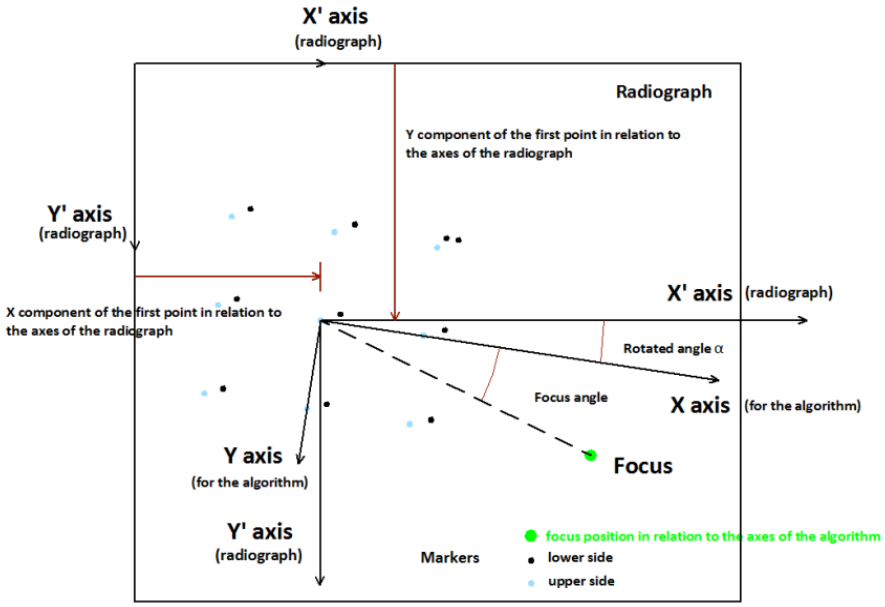

Figure 9. Representation of focus position on radiograph

Finally, it´s enough to add the two known vectors (figure 10) to know the position of the origin of relative system, with regard to the X-ray emitting focus.

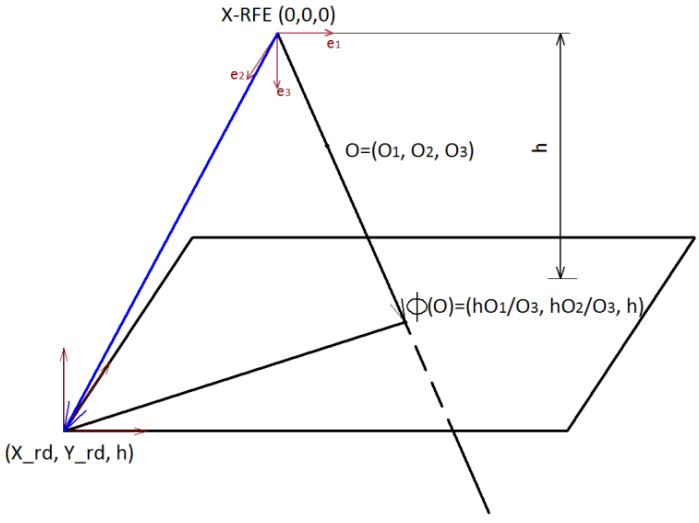

Figure 10. Calculation method of coordinates of the upper left corner of image in relation to the focus

3. Results

The inability to use geometric points as markers in practice [22], forced us to validate model accuracy experimentally under real use conditions with markers that are made up of small spheres, in order to determine the order of magnitude of the mistakes that this could cause. For that purpose, four series of tests were designed, the first three with synthetic radiographs, and the last series with real radiographs. This analysis methodology, using images both from virtual models and radiographs has previously been used for other experiments of identifying medical images with other techniques [23]. Obviously, in virtual tests, the exact position of the X-ray focus is known, so its position error can be calculated easily. On the other hand, it is necessary to mention that the set of obtained samples follows a normal distribution, so $[\mu-k\sigma, \mu+k\sigma]$ interval corresponds to 99.5% of the values for k=2.578.

3.1. First series of tests

The influence in final result of the selection of a set of four markers or other in radiograph was studied [24,25], and for this purpose, four synthetic radiographs were generated. Three mistake-estimate parameters were considered like in the rest of tests: the coordinates of focus determined, the coordinates of the first chosen marker that allowed to verify that mistakes show no characteristic pattern, and the resolution of radiographic image. Furthermore, fourteen different combinations of the four markers needed were selected in each synthetic radiograph to calculate the spatial position of focus, these combinations being equals in the four radiographs. A total of 56 tests were performed.

One of the four analyzed synthetic radiographs was generated with the following parameters:

h = 764,8mm O = (-46, -61, 469´5)

Resolution = 4 pixels/mm

(X_rd, Y_rd) = (-177´25, -214´875)

The results in the other three radiographs, generated with completely different parameters to the first one, were similar.

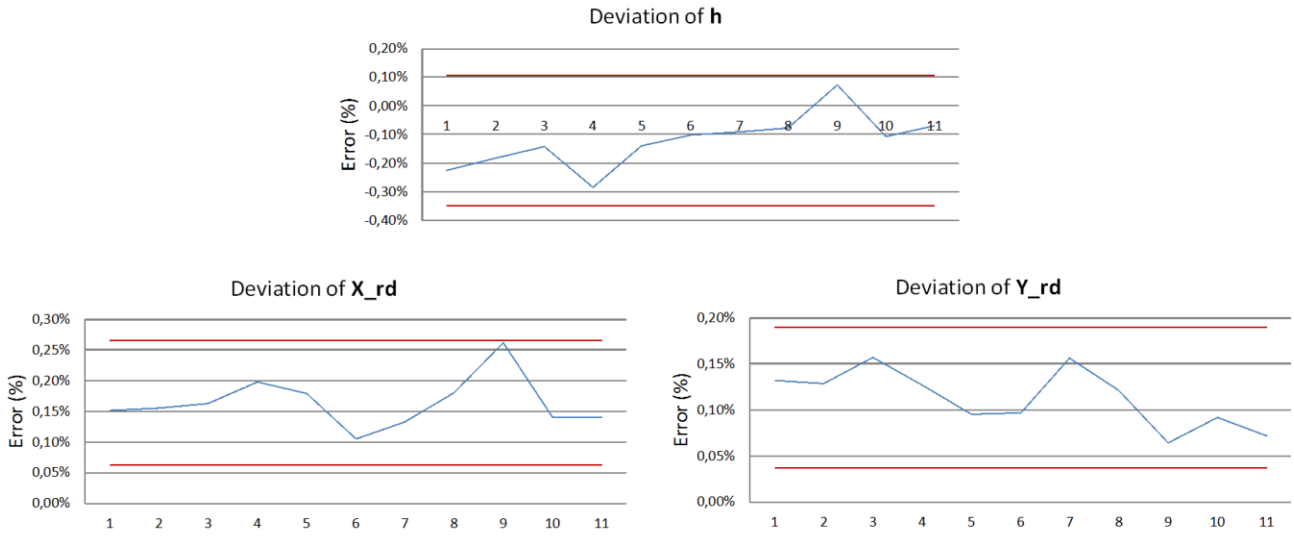

Figure 11. Error in the calculation of focus coordinates depending on selected markers

Results of the first eleven combinations of the set of four markers show 99, 5% of the values are within a range of maximum error of [-0,35%, +0,39%] which is considered acceptable. Error variation in the height of the focus from the radiograph in relation to the exact position of focus does not exceed 0.3% in the confidence interval, leaving the maximum measured error in just over 2 mm in this case.

The exact position of the first chosen marker is known in virtual tests, as it was said, and we can study its position error in order to look for possible patterns. In all tests that were performed, it was verified that there is no correlation between the error variation curves. As expected, it can be observed that there is a correlation between the position errors of this marker and those of the focus. There is no an appreciable error pattern in X and Y coordinates of the focus position either.

In the last three combinations of set of markers, the third and fourth selected markers were placed in the same vertical line and this case has no solution as it was already said.

The implemented program prevents this situation beforehand by warning with an error message.

3.2. Second series of tests

The influence on the final result of the focus position variation in relation to the radiograph in the directions of the X, Y and Z axes was studied. In specific, fifteen variations of position were considered for each axis of the coordinates, which were taken in increments of five millimeters over a range of ± 30mm, together with two other cases at distances of ± 50mm in order to check the behavior in the most remote areas. In Z axis, two more cases were added at distances of ±100 millimeters in relation to initial position. A total of 47 tests were performed in this series. In all cases the same markers were chosen in order to not to introduce any additional factor that could influence in result.

As an example, the results when the focus of X-ray machine is moved in Y axis direction are shown. Results in the other two directions were similar. The radiograph was generated with the following parameters:

h = 1200 mm O = (-50, -60, 900)
Resolution = 5 pixels/mm
(X_rd, Y_rd) = (-166, -220)

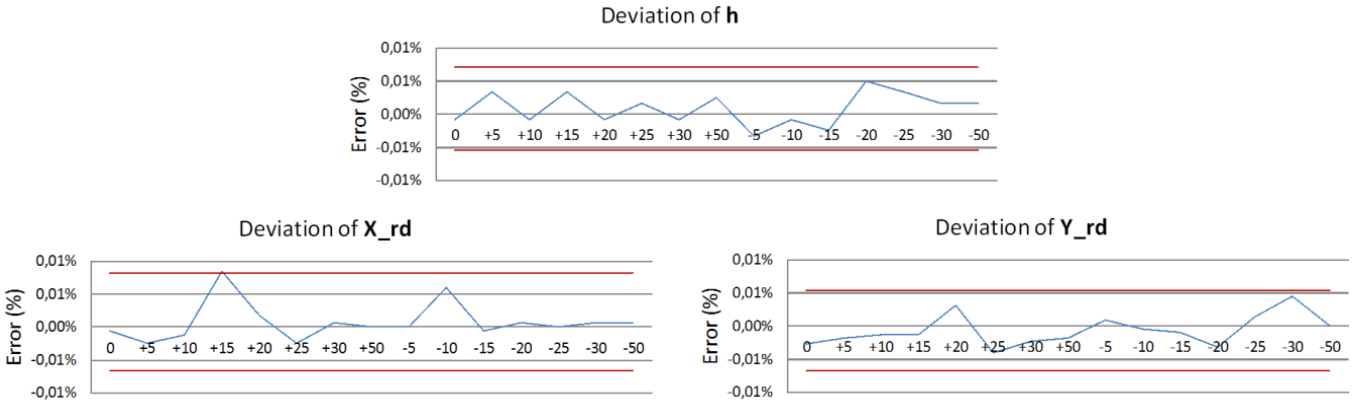

Figure 12. Error in the calculation of focus coordinates when the focus is moved in the Y axis direction

The results in the fifteen positions clearly show that expected error for 99.5% of the values considered is in a range of maximum error of [-0.03%, +0.02%], so that, the influence on the result of the variation of the focus position in Y axis is practically null. The result of the error for h was, in all cases, lower than in the first series, as it in no case exceeded 0.01%, which was expected because there are no restrictions or dependences in the model regarding the focus position. As in the first series, no correlation was found between the percentage of position errors of the reference marker and the position errors in X and Y are also less than 0.01% in all test cases.

3.3. Third series of tests

The influence on the final result of the possible rotated angle (α) about Z axis (the only axis is possible for a turn to take place in the normal real use of the locator object, which is set on a table of the x-ray machine) between the axes of the reference systems used, was studied. Angular variations of 15° in a range between 0° and 90° were considered first. To ensure the reliability of the model, regardless of the angle at which the locator object is rotated, a second analysis was made by turning the locator object an angle of 360° in intervals of 30°. Finally, since in practice it is not feasible to turn the locator object 360°, a third study was performed at angular intervals of 5° within ± 15°. It was necessary to consider the possibility of turning the locator object 180°. As in the previous case, the same markers were always chosen.

In this section, the results by rotating the locator object 360º at 30º intervals are shown. The results in the rest of the tests were similar. Initial radiograph was generated with the following parameters:

h = 1200 mm O = (-50, -60, 900)
Resolution = 5 pixels/mm
(X_rd, Y_rd) = (-166, -220)

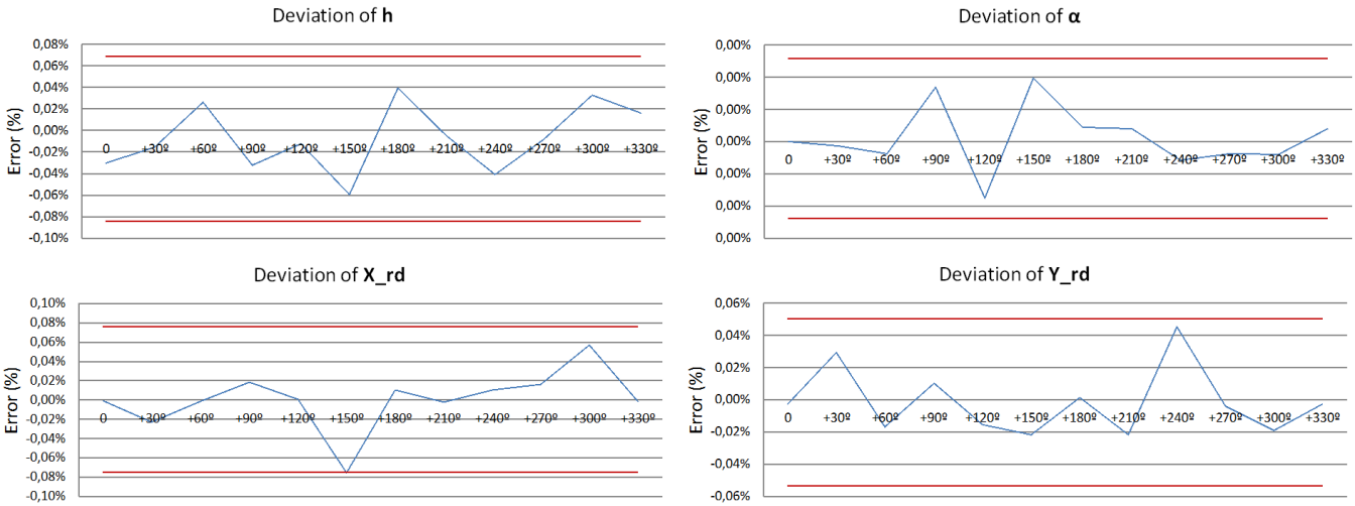

Figure 13. Error in the calculation of α and focus coordinates when the locator object is rotated

The results in the twelve radiographs show that the expected error for 99.5% of the values is in a range of maximum error of ± 0.12%, which is considered acceptable.

As expected, because of the trigonometric functions that implement programming languages, results of the error for h, show a relatively high error. This is because we must add this error to the signaling error, which increases the mean measure to a maximum of 0.06%, greater than that measured in the second series.

Like the position errors of the reference marker, there is nothing different to note in this series of tests, nor errors of X and Y. Results of α error were illustrated in figure 13, as α is a value which influences on calculus of radiograph position in relation to focus.

3.4. Fourth series of tests

Previous series of tests confirmed the effectiveness and accuracy of the proposed model using spherical markers [26]. However, a last series of tests was performed with real radiographs using a standard equipment for clinical use. Real radiographs were made only with the locator object, without the presence of the patient, because any movement of the latter could falsify the results. As it is not possible to use the real focus position in relation to the radiograph, in order to estimate the error, a first position was accepted as actual focus position, which was calculated by LEFERX software. Afterwards, the

focus of the X-ray machine was moved precise known distances in the three space coordinates and it was proven that differences between calculated solutions matched up with displacements that were done. Series of ten radiographs were made in each space coordinate at intervals of 10 millimeters each, so the range of variation between the first and the last one was 90 millimeters.

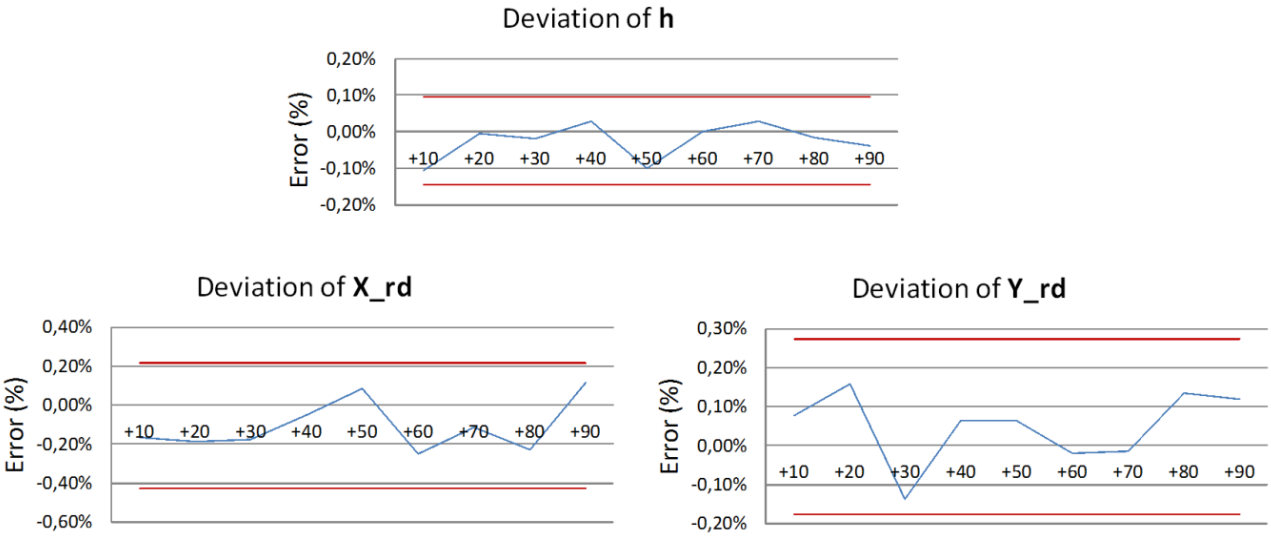

Figure 14. Error in the calculation of focus coordinates when the focus is moved in the Z axis direction

Results show 99.5% of the values are within a range of maximum error of [-0.23%, +0.17%] which is considered acceptable.

Results in all tests that were performed in the first experimental series, suggest the validity, in practice, of the proposed model and allow to affirm that small variations in the signaling of the centers of real markers generates minimal alterations in the result, and also that, the selection of the four markers is independent of the method accuracy.

Based on results of second series of tests, it can be stated that the influence on the result of the variation of the focus position in the three coordinate axes is practically null and the independence of the geometric model is guaranteed in relation to the focus position.

Results of the third series of tests proved the independence of the geometrical model in relation to the focus orientation on radiographs. On the other hand, the results of tests on

real radiographs hardly differed from those made on virtual radiographs, in relation to the error range of the coordinates. Therefore, it can be concluded that if tantalum markers which diameter is 0.5 mm are used, then it will be possible to ensure that the maximum error in each coordinate of the focus position on the radiograph will not exceed 0.8%. Accuracy is high enough to state that the geometric model that was proposed is reliable and accurate. Also, it can be said that the locator object prototype that was manufactured performs the objectives that were set initially, providing the necessary information to calculate the position of the focus in space.

4. Discussion

Taking measurements on standard radiographs is a common method used in preoperative planning and postoperative surveillance in biomechanics field. Biomechanical studies made from radiological images are safe, versatile and economical but today, they suffer from poor precision [14,27], although an automated measurement method is used [28], which limits their field of application.

In this paper, we present a novel geometric model based on projections in order to calculate accurately, practically and economically, the exact position of the focus required to perform accurate measurements over radiographs. The model was implemented as a practical computer program by a multidisciplinary group of engineers, providing a useful and friendly tool which can be used with any standard radiographic system, that is, a system available in any hospital. It is important to highlight that this model can be applied in systems with a single focus and a single radiographic image. A novel reference locator object was also designed and manufactured, which avoids introducing markers inside the human body. Model effectiveness was demonstrated by performing virtual simulations with synthetic radiographs prior to performing tests with

real radiographs. After real tests, whose excellent results in obtaining the exact focus position were similar to virtual ones, it can be proved the accuracy is high enough to guarantee the proposed model is reliable and precise.

As previously discussed, CT or RSA techniques are used in preoperative planning and postoperative surveillance of several arthroplasties, for example hip or knee. Both techniques expose the patient to high doses of radiation and carry high cost. We are seeing an increase in use of CT scans for planning purposes in knee arthroplasty. These scans are often used with little consideration or understanding of the associated risks of radiation exposure which is 100 to 1000 times higher than that associated with conventional radiography. CT examinations may pose a measurable risk to patients and as a high dose imaging modality, the medical community aims to limit its use [15].

On the other hand, estereoradiological analysis techniques were developed over 40 years ago in trauma studies to measure the skeletal system using pairs of radiographs made simultaneously [29]. RSA is a high-accuracy method to evaluate movement between fixed bony structures and to measure their wear [30], in addition to knowing the existing motion between the implant and the host bone from their radiographs. Björk [31] improved this technique by inserting a series of metallic spheres of known dimensions, called markers, into bone tissue in order to establish a radiographic reference for evaluating changes in the position of the bone tissue to be studied. Finally, Selvik established the practical basis of this technique, although its principal application focuses on the evaluation of joint prostheses [32]. Some researchers have replaced these markers with the three-dimensional data provided by a CT scan. However, the results show significantly lower accuracy than with markers [22]. Still today, alternatives are being sought to prevent the introduction of foreign elements into the human body. Selvik determined that the most appropriate markers are small spheres of tantalum as

this material is biocompatible. These spheres are held in a fixed position and they do not produce any adverse effects on the patient. Once radiographs are taken, the markers are displayed with great sharpness and they are useful as a spatial positioning reference for the components that they host. Although tests have been made with other materials such as bioactive glass [33], the tantalum provides better results.

The practical development of RSA techniques has highlighted the difficulty of determining the exact points of emission of X-rays [19], this determination being essential for mathematical models to avoid excessive data errors. Therefore, the technique requires the use of a reference-marker locator object of known geometry that calculates the coordinates of these emission sources in relation to a global reference system. Calibration methods can be used for this purpose [26,34].

The complexity of RSA imaging results in higher exposure repetition rates [35,36]. The number of exposures directly reflects the radiation dose delivered to the patient; so, the less exposures used to obtain a useful image pair that satisfies RSA image criteria, the less the risk of stochastic damage later in the patient's life. The exposure is done with two x-ray tubes simultaneously, so the dose of radiation delivered to the patient during RSA imaging is double compared to a standard x-ray exposure of the same anatomical region. Exposure repetition and image evaluation during RSA imaging is time consuming, and RSA examination time can be long (up to one hour).

Another important drawback of the RSA technique is its high cost, since it cannot be implemented in commercial X-ray systems.

Nowadays, it is sought that new methods reduce radiation dose and costs in RSA. Recent publications have shown there is strong evidence that implementation of RSA personalized patient protocols has a positive effect on radiation dose savings. Radiographers treating patients equipped with a personalized patient protocol achieved

significantly shorter examination time and a reduced number of exposures, when compared to the control group using a standard RSA protocol, thus ensuring a cost benefit for department and patient safety [16]. The implementation of our model will improve both radiation dose and costs.

Regarding to reduction of dose radiation in CT, a recent publication has used a statistical content-adapted sampling for 3D X-ray Computed Tomography imaging using a few 2D projection data. The obtained results indicates that the creation of an adapted sampling in low dose computed tomography is reachable and it could be use in medical applications, such as the design of patient-specific prosthetic or the surveillance of pathologies that require medical monitoring over a long period of time. Using fewer projections comparing with current CT, practitioners may evaluate the evolution of the pathology by computing the deformation field between previous and current examinations, although higher doses of radiation are needed than in conventional x-rays as the first CT scan must be performed at complete dose to create a high resolution surface model [37].

Recent studies have also found patient characteristics that are associated with higher radiation burden from CT imaging which allows to target efforts towards dose reduction more effectively [39].

On the other hand, there are recent studies which propose the creation of a composite image from multiple x-ray images, taken at different exposure times. This image is created in analogy to visible-light high dynamic range photography. This new x-ray imaging method promises to acquire and store contrast in a wider range of densities than conventional single-exposure x-ray images. Due to the higher amount of detail encoded in an enhanced dynamic range x-ray image, it is expected that the number of retaken images can be reduced, and patient exposure overall reduced [38].

The diagnostic information of an enhanced dynamic range x-ray image can be placed somewhere between conventional x-rays and CT. The tissue discrimination of CT is many times higher than that of conventional x-rays, but an enhanced dynamic range x-ray improves tissue discrimination over conventional x-rays predominantly in the presence of large contrast gradients. Compared with CT, however, radiation exposure is much lower, namely in the range of a conventional x-ray image. Moreover, the cost of modified x-ray equipment can be expected to be similar to that of conventional x-ray devices and therefore much cheaper than CT or even magnetic resonance imaging.
It is also envision that the use of high dynamic range projections can improve dual energy absorptiometry and even computed tomography by reducing the number of low-exposure ("photon-starved") projections.

5. Conclusions and future work

In view of the results, it can be concluded that it was possible to establish a valid geometric model based upon projections that allow to determine accurately the position, in space, of the X-ray emitting source of any standard commercial radiographic system. It was possible to prove that the proposed model can be implemented like a computer algorithm, useful in practice, that only requires a digital or digitized standard radiograph to work. It could also be shown that it is possible to manufacture a reference locator object, according to the requirements of the proposed model, to apply this model in practice. This work will make it easier to perform economical and non-invasive postoperative surveillance, reducing waiting times.
Two indirect contributions of this research to the biomechanics field must be highlighted. The first is the interest that exists within the scientific community to determine with precision the wear of the plastic components of modern implants using

standard radiographs. As it was said, in practice, there is no way to predict that wear without knowing with great accuracy and economy, the position of the X-ray focus. Secondly, this study has contributed to the creation of a commercial product that is currently under development. The end of the entire process will simply provide these three numbers, the X, Y and Z coordinates of the X-ray focus.

On the other hand, this study reveals three main future lines of research. The first will be to study how to automate the process of selecting markers on radiographs. In practice, this process is the main source of error and, despite it was shown that this error is insignificant, it will be necessary to study it, to try to reduce it to a minimum. It was also seen, that perhaps, it is possible to reduce the error by modifying the shape of the tantalum markers. It is only possible to get them in market with spherical shape but if they had a sharp vertex, it would be possible to point them out with more precision than the center of a disk, as currently happens. Finally, it would be desirable to be able to dispense with the locator object or replace it with a virtual locator to apply the proposed methodology with greater flexibility.

Competing interests

None declared.

Acknowledgements

This work was funded by research project of Oviedo University (Spain) called "*Metodología integral de localización radiográfica de sistemas de interposición acetabular para implantación ósea directa mILR*" which reference is FOU-EM-126-12.

We would like to thank the San Agustin hospital (Spain) by providing technical assistance in the performing of radiographs and particularly to Daniel Hernández (head of traumatology service) for his support and involvement in field tests of this work.

References

[1] S.M. Zingde, J. Slamin

Biomechanics of the knee joint, as they relate to arthroplasty

Orthopaedics and Trauma, 31 (1) (2017), pp. 1-7

doi.org/10.1016/j.mporth.2016.10.001

[2] F. Castagnini, A. Sudanese, B. Bordini, E. Tassinari, S. Stea, A. Toni

Total Knee Replacement in Young Patients: Survival and Causes of Revision in a Registry Population

The Journal of Arthroplasty, 32 (11) (2017), pp. 3368-3372

doi.org/10.1016/j.arth.2017.05.052

[3] F. Canovas, L. Dagneaux

Quality of life after total knee arthroplasty

Orthopaedics & Traumatology: Surgery & Research 104 (1) (2018), pp. S41-S46

doi.org/10.1016/j.otsr.2017.04.017

[4] A.W. Glover, A.J.A. Santini, J.S. Davidson, J.A. Pope

Mid-to long-term survivorship of oxidised zirconium total knee replacements performed in patients under 50 years of age

The Knee (2018)

doi.org/10.1016/j.knee.2018.03.014

[5] W.M. Oliver, C.H.C. Arthur, A.M. Wood, R.A.E. Clayton, I.J. Brenkel, P. Walmsley

Excellent Survival and Good Outcomes at 15 Years Using the Press-Fit Condylar Sigma Total Knee Arthroplasty

The Journal of Arthroplasty, (2018) pp. 1-6

[6] R. Vaishya, V. Vijay, D.M. Demesugh, A.K. Agarwal

Surgical approaches for total knee arthroplasty

Journal of Clinical Orthopaedics and Trauma, 7(2) (2015), pp. 71-79. doi.org/10.1016/j.jcot.2015.11.003.

[7] B.J. McGrory, C.D. Etkin, D.G. Lewallen

Comparing contemporary revision burden among hip and knee joint replacement registries

Arthroplasty Today, 2 (2) (2016), pp. 83-86

doi.org/10.1016/j.artd.2016.04.003

[8] L. Zach, L. Kunčická, P. Růžička, R. Kocich

Design, analysis and verification of a knee joint oncological prosthesis finite element model

Computers in Biology and Medicine, 54 (1) (2014), pp. 53-60

doi.org/10.1016/j.compbiomed.2014.08.021

[9] S. Lasurt-Bachs, P. Torner, F. Maculé, E. Prats, F. Menéndez-García, J. Ríos-Guillermo, A. Torrents

Cross-linked polyethylene does not reduce wear in total knee arthroplasty

Revista española de cirugía ortopédica y traumatologia, 62 (3) (2018), pp. 197-203.

doi.org/10.1016/j.recote.2018.03.004

[10] H. Haider

Reference Module in Materials Science and Materials Engineering

Comprehensive Biomaterials II, 7 (2017), pp. 152-174

doi.org/10.1016/B978-0-12-803581-8.09359-0

[11] A.L.L. Oliveira, E.G. Cueva, R.T. Carvalho

Failure analysis of the tibial component baseplate after total knee arthroplasty

Engineering Failure Analysis , 36 (2014), pp. 147-154

doi.org/10.1016/j.engfailanal.2013.10.012

[12] A.C. Peek, B. Bloch, J. Auld

How useful is templating for total knee replacement component sizing?

The Knee, 19 (4) (2012), pp. 266-269

doi.org/10.1016/j.knee.2011.03.010

[13] M. Ettinger, L. Claassen, P. Paes, T. Calliess

2D versus 3D templating in total knee arthroplasty

The knee, 23(1) (2016), pp. 149-151

doi.org/10.1016/j.knee.2015.08.014

[14] C.D. Stickley, J.J. Wages, R.K. Hetzler, S.N. Andrews, C.K. Nakasone

Standard radiographs are not sufficient for assessing knee mechanical axis in patients with advanced osteoarthritis

The journal of arthroplasty, 32 (2017), pp. 1013-1017

doi.org/10.1016/j.arth.2016.09.024

[15] D.Y. Ponzio, J.H. Lonner

Preoperative mapping in unicompartental knee arthroplasty using computed tomography scans is associated with radiation exposure and carries high cost

The journal of arthroplasty, 30 (6) (2015), pp. 964-967

doi.org/10.1016/j.arth.2014.10.039

[16] O. Muharemovic, A. Troelsen, M.G. Thomsen, T. Kallemose, K.K. Gosvig

The effect of personalized versus standard patient protocols for radiostereometric analysis (RSA)

Radiography, 24 (2) (2018), p. e31-e36

doi.org/10.1016/j.radi.2017.11.006

[17] E.H. Garling, B.L. Kaptein, K. Geleijns, R.G.H.H. Nelissen, E.R. Valstar

Marker Configuration Model-Based Roentgen Fluoroscopic Analysis

Journal of Biomechanics, 38(4) (2005), pp. 893-901

doi: 10.1016/j.jbiomech.2004.04.026

[18] E.H. Barry, H.W. Eves

Introducción a las transformaciones geométricas

Mexico: Compañía Editorial Continental (1976)

[19] R. Madanat, N. Moritz, H.T. Haro

Three-dimensional computer simulation of radiostereometric analysis (RSA) in distal radius fractures

Journal of Biomechanics, 40(8) (2007), pp. 1855-1861

doi.org/10.1016/j.jbiomech.2006.07.004

[20] S. Attaway

MATLAB: a practical introduction to programming and problem solving (2nd Ed)

Massachussets (USA): Elsevier (2012)

[21] M.B. Williams, E.A. Krupinski, K.J. Strauss, W.K. Breeden, M.S. Rzeszotarski, K. Applegate, M. Wyatt, S. Bjork, J.A. Seibert

Digital radiography image quality: Image acquisition

Journal of the American College of Radiology, 4(6) (2007), pp. 371-388

doi: 10.1016/j.jacr.2007.02.002

[22] P.W. De Bruin, B.L. Kaptein, B.C. Stoel, J.H.C. Reiber, P.M. Rozing, E.R. Valstar

Image-based RSA: Roentgen stereophotogrammetric analysis based on 2D–3D image registration

Journal of Biomechanics, 41(1) (2008), pp. 155-164

doi: 10.1016/j.jbiomech.2007.07.002

[23] M.S. Emami, K. Omar (2013)

A low-cost method for reliable ownership identification of medical images using SVM and Lagrange duality

Expert systems with applications, 40(18) (2013), pp. 7579-7587

doi: 10.1016/j.eswa.2013.07.062

[24] R.Y. Cai, X.H. Yuan, C. Rorabeck, R.B. Bourne, D.W. Holdsworth

Development of an RSA calibration system with improved accuracy and precision

Journal of Biomechanics, 41(4) (2008), pp. 907-911
doi: 10.1016/j.jbiomech.2007.11.012

[25] J. Ioppolo, N. Borlin, C. Bragdon, M. Li, R. Price, D. Wood, H. Malchau, B. Nivbrant
Validation of a low-dose hybrid RSA and fluoroscopy technique: Determination of accuracy, bias and precision
Journal of Biomechanics, 40 (3) (2007), pp. 686-692.
doi: 10.1016/j.jbiomech.2006.01.012.

[26] M Gammunto, S. Martelli, C. Trozzi, L. Bragonzoni & A. Russo
A simulation environment for estimation of the performance of RSA cages
Computers in Biology and Medicine, 38(9) (2008), pp. 1000-1006
doi: 10.1016/j.compbiomed.2008.07.007

[27] V. Sarwahi, S. Ayan, T. Amaral, S. Wendolowski, R. Gecelter, Y. Lo, B. Thornhill
Can postoperative radiographs accurately identify screw misplacements?
Spine deformity, 5(2) (2017), pp. 109-116
doi.org/10.1016/j.jspd.2016.10.007

[28] W. Wojciechowski, A. Molka, Z. Tabor
Automated measurement of parameters related to the deformities of lower limbs based on x-rays images
Computers in Biology and Medicine, 70 (2017), pp. 1-11
doi.org/10.1016/j.compbiomed.2015.12.027

[29] S. Ci-Bin, L. Jiing-Yih, C. Ren-Yi, S. Kao-Shang, C. Kuo-Jen, L. Shang-Chih
Automatic model-based roentgen stereophotogrammetric analysis (RSA) of total knee prostheses
Journal of Biomechanics, 45(1) (2012), pp. 164-171
doi.org/10.1016/j.jbiomech.2011.09.011

[30] S. Imai, K. Higashijima, A. Ishida, Y. Fukuoka, A. Hoshino, H. Minamitani
Determination of the position and orientation of artificial knee implants using markers embedded in a bone: preliminary in vitro experiments
Medical Engineering & Physics, 25(5) (2003), pp. 419-424
doi: 10.1016/S1350-4533(03)00037-7

[31] A. Bjork
Facial growth in man studied with the aid of metallic implants
Acta Odontologica Scandinavica, 13 (1995), pp. 9-34
doi: 10.3109/00016355509028170

[32] L. Montagna, L. Bragonzoni, M.L. Zarnpagni, A. Russo, M. Motta, U. Albisinni, M. Marcacci

Investigation into the detection of marker movement by biplanar RSA

Medical Engineering & Physics, 27(8) (2005), pp. 641-648

doi: 10.1016/j.medengphy.2004.12.004

[33] R. Madanat, N. Moritz, E. Vedel, E. Svedström, H.T. Aro

Radio-opaque bioactive glass markers for radiostereometric analysis

Acta Biomaterialia, 5(9) (2009), pp. 3497-3505

doi: 10.1016/j.actbio.2009.05.038

[34] A.M.T. Choo, T.R. Oxland

Improve RSA accuracy with DLT and balanced calibration marker distributions with an assessment of initial-calibration

Journal of Biomechanics, 36(2) (2003), pp. 259-264

doi: 10.1016/S0021-9290(02)00361-5

[35] O. Muharemovic, A. Troelsen, M.G. Thomsen, T. Kallemose, K.K. Gosvig

A pilot study to determine the effect of radiographer training on radiostereometric analysis imaging technique

Radiography, 24(2) (2018), pp. e37-e43

doi.org/10.1016/j.radi.2017.12.003

[36] O. Muharemovic, A. Troelsen, M.G. Thomsen, T. Kallemose, K.K. Gosvig

Design and evaluation of learning strategies for a group of radiographers in radiostereometric analysis (RSA)

Radiography, 23(4) (2017), pp. e80-e86

doi.org/10.1016/j.radi.2017.05.015

[37] A. Cazasnoves, S. Sevestre, F. Buyens, F. Peyrin

Statistical content-adapted sampling (SCAS) for 3D computed tomography

Computers in Biology and Medicine, 92(1) (2018), pp. 9-21

doi.org/10.1016/j.compbiomed.2016.11.001

[38] M.A. Haidekker, L. Dain-kelley Morrison, A. Sharma, E. Burke

Enhanced dynamic range x-ray imaging

Computers in Biology and Medicine, 82(1) (2017), pp. 40-48

doi.org/10.1016/j.compbiomed.2017.01.014

[39] J.N. Cooper, D.L. Lodwick, B. Adler, C. Lee, P.C. Minneci, K.J. Deans

Patient characteristics associated with differences in radiation exposure from pediatric abdomen-pelvis CT scans: A quantile regression analysis

Computers in Biology and Medicine, 85 (2017), pp. 7-12

doi.org/10.1016/j.compbiomed.2017.04.003